Mechanics and Mechanical Engineering
Vol. 7, No. 1 (2004) 133–152

Stability Analysis of Rotor-Bearing Systems via Routh-Hurwitz Criterion

Abd Alla EL-MARHOMY
Department of Engineering, Mathematics and Physics, Faculty of Engineering,
Ain Shams University
Cairo, Egypt

Received (9 September 2003)
Revised (4 October 2003)
Accepted (3 December 2003)

A method of analysis is developed for studying the whirl stability of rotor-bearing systems without the need to solve the governing differential equations of motion of such systems. A mathematical model comprised of an axially symmetric appendage at the mid span of a spinning shaft mounted on two dissimilar eight-coefficient bearings is used to illustrate the method. Sufficient conditions for asymptotic stability of both the translational and rotational modes of motion of the system have been derived. The system stability boundaries presented graphically in terms of the various system non-dimensionalized parameters afford a comprehensive demonstration of the effects of such parameters on system stability of motion.

Keywords: rotor-bearing system, stability, Hurwitz, Routh.

1. Introduction

In spite of the fact that the subject of dynamics and stability of rotor-bearing systems has been the concern of engineers and scientists for more than a century, it will persist as an active area of research and study for the foreseeable future. This may be attributed to its various applications in many modern fields in addition to the increasing trend toward ultra-high speeds in rotating machinery. For an inclusive historical background and a comprehensive literature review on the subject see [1].

The common approach adopted for investigating stability of rotor-bearing systems in most of the relevant literature depends mainly upon solving the set of system governing equations of motion after being simplified under certain assumptions and after being transformed into an eigenvalue problem. Then, from the solution of the exponential growth (unstable) or decay (stable). the stability criteria are established based on the resulting eigenvalues and their system parametric dependence. Typical studies are [2] to [6]. As obvious from literature review, it is a common feature in the rotor-bearing problems that the resulting governing deferential equations

of motion of the system are so difficult and complex that seeking their analytical solution is always tough task if not impossible unless major simplifications and assumptions are imposed on them.

The main motivation for this work is to gain an inclusive understanding of the role played by each of the various system parameters on the whirl stability of its motion without solving the resulting tough set of governing differential equations of motion. This objective has been actualized by adopting Routh-Hurwitz criterion as a simple technique, which can afford a solution to the question of stability of motion of linear autonomous dynamical systems without solving the corresponding governing differential equations of motion. The stability analysis has been performed on a rotor-bearing system modeled as an axially symmetric appendage at the mid span of a spinning shaft mounted on two dissimilar 8-coefficient end bearings. The governing differential equations of motion of the system have been derived. The coupling between the translational and rotational modes of motion has been eliminated after linearizing the system equations of motion. Routh-Hurwitz criterion has been applied on each mode to get sufficient conditions of asymptotic stability of whirling motion of the system. Based on the developed stability conditions, the system stability regions were illustrated graphically in terms of the various system non-dimensionalized parameters.

2. Problem Formulation

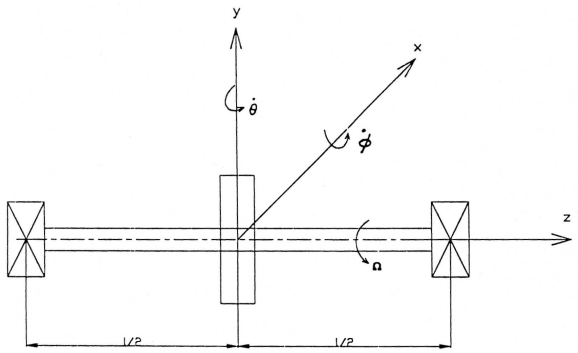

Figure 1 Appendage-shaft-bearing model

The mathematical model as depicted in Fig. 1 consists of a disk (or generally an axially symmetric appendage) which mass m^* at the mid span of a spinning shaft of length l and mass m mounted on a pair of massless dissimilar nonlinear 8-coefficient bearings (Fig. 2). It is assumed that

1. the shaft is straight, balanced, rigid and axially symmetric,
2. the system's rotational and translational displacements are small,
3. axial and torsional constraints are negligible,

4. aerodynamic effects are not included, and,
5. the static deflections are negligible compared to the dynamic effects.

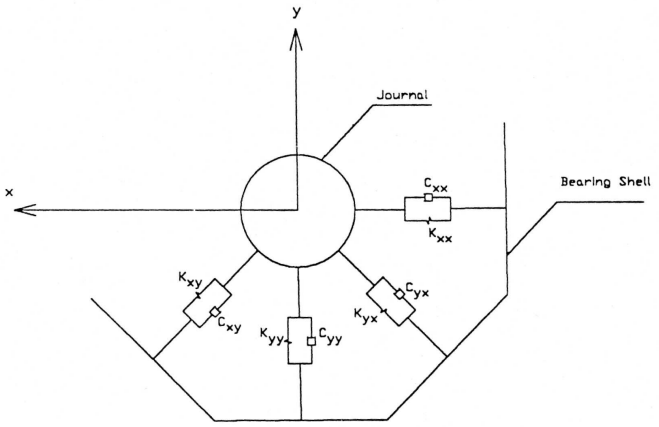

Figure 2 8-coefficient bearing model

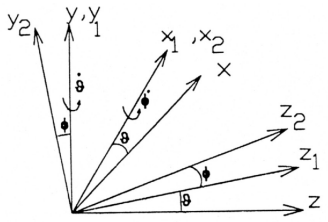

Figure 3 Shaft coordinate axes

In the dynamic equilibrium configuration of the system, the shaft centerline is considered to be along the Z-direction of a rotating X, Y, Z coordinate system described by unit vectors $\bar{i}$, $\bar{j}$, $\bar{k}$. Due to the flexibility of the two end bearings. the center of mass of the system is going to translate in the $\bar{i}$ and $\bar{j}$ directions with the infinitesimal displacements x and y respectively, and the shaft-appendage system is going to rotate with the angular velocities $\dot{\phi}\bar{i}$ and $\dot{\theta}\bar{j}$ in addition to the spinning velocity $\Omega\bar{k}$. The coordinate system transformations used for the formulation of the problem kinematics is illustrated in Fig. 3. The position vector $\bar{r}(z,t)$ of a typical differential element at a distance z from o along the shaft can be written as:

$$\bar{r}(z,t) = x(z,t)\bar{i} + y(z,t)\bar{j}\,. \tag{1}$$

The resultant angular velocity $\bar{\omega}$ of the shaft is

$$\bar{\omega} = \bar{\Omega} + \dot{\bar{\theta}} + \dot{\bar{\phi}}\,, \tag{2}$$

which can be written as

$$\bar{\omega} = \left(\dot{\phi} - \theta\Omega\right)\bar{i} + \left(\dot{\theta} - \phi\Omega\right)\bar{j} + \left(\Omega + \theta\dot{\phi}\right)\bar{k}\,, \tag{3}$$

where θ and ϕ are the shaft infinitesimal rotational displacements in the $(x-z)$ and $(y-z)$ planes respectively as depicted schematically in Fig. 4.

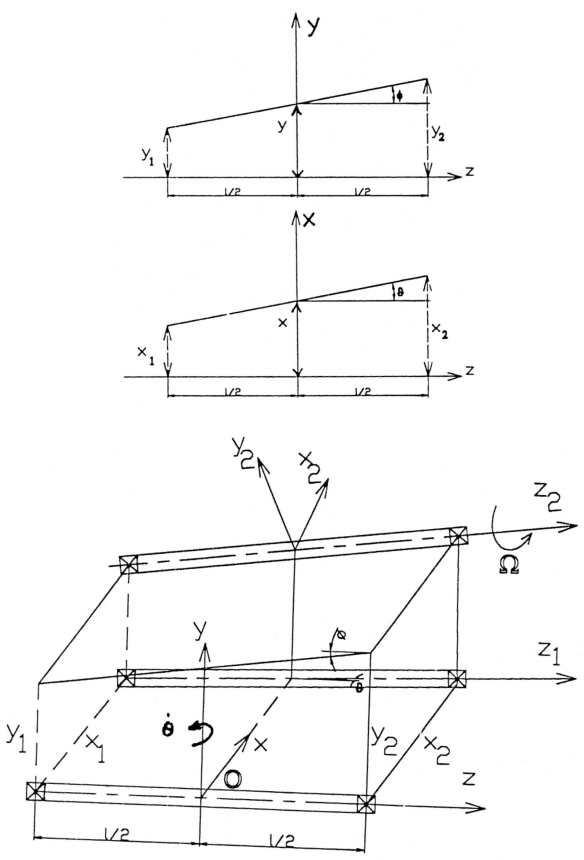

Figure 4 Schematic diagram illustrating the translational and rotational displacements

Differentiating Eq. (1) with respect to time, the velocity vector $\dot{\bar{r}}(z,t)$ is

$$\dot{\bar{r}}(z,t) = \left[\dot{x} - y\Omega - y\theta\dot{\phi}\right]\bar{i} + \left[\dot{y} + x\Omega + x\theta\dot{\phi}\right]\bar{j} + \left[y(\dot{\phi} - \theta\Omega) - x(\dot{\theta} - \phi\Omega)\right]\bar{k}\,. \tag{4}$$

The kinematic energy of the system T can then be obtained as:

$$\begin{aligned} T &= \frac{1}{2}(m+m^*)\left\{\dot{x}^2+\dot{y}^2+x^2\dot{\theta}^2+y^2\dot{\phi}^2+2\dot{\phi}(x\dot{y}-y\dot{x})-2xy\dot{\theta}\dot{\phi}+\right. \\ &\quad \left. 2\Omega\left[x\dot{y}-y\dot{x}+x^2(\theta\dot{\phi}-\phi\dot{\theta})+xy(\theta\dot{\theta}+\phi\dot{\phi})\right]+\Omega^2\left[x^2+y^2\right]\right\}+ \\ &\quad \frac{1}{2}(I_d+I_d^*)\left\{\dot{\theta}^2+\dot{\phi}^2-2\Omega(\theta\dot{\phi}+\phi\dot{\theta}\right\}+\frac{1}{2}(I_p+I_p^*)\left(\Omega^2+2\Omega\theta\dot{\phi}\right), \end{aligned} \tag{5}$$

where I_d and I_d^* are the diametral mass moment of inertia of shaft and disk respectively where I_p and I_p^* are the polar ones. The strain energy of the bearing systems is [7]:

$$\begin{aligned} V &= \frac{1}{2}\left[\left(K_{x_1x_1}x_1^2+K_{x_1y_1}x_1y_1+K_{y_1x_1}y_1x_1+K_{y_1y_1}y_1^2\right)+\right. \\ &\quad \left.\left(K_{x_2x_2}x_2^2+K_{x_2y_2}x_2y_2+K_{y_2x_2}y_2x_2+K_{y_2y_2}y_2^2\right)\right], \end{aligned} \tag{6}$$

in which K_{xx} and K_{yy} are the principal (direct) stiffness coefficients of the bearing, K_{xy} and K_{yx} are the cross coupling stiffness coefficients, x and y denote the deflections of the bearing center and the subscripts 1 and 2 refer to the left and right bearing respectively. The Rayleigh's dissipation energy of the bearing system is [8]:

$$\begin{aligned} D &= \frac{1}{2}\left[\left(C_{x_1x_1}\dot{x}_1^2+C_{x_1y_1}\dot{x}_1\dot{y}_1+C_{y_1x_1}\dot{y}_1\dot{x}_1+C_{y_1y_1}\dot{y}_1^2\right)+\right. \\ &\quad \left.\left(C_{x_2x_2}\dot{x}_2^2+C_{x_2y_2}\dot{x}_2\dot{y}_2+C_{y_2x_2}\dot{y}_2\dot{x}_2+C_{y_2y_2}\dot{y}_2^2\right)\right], \end{aligned} \tag{7}$$

where C_{xx} and C_{yy} are the bearing principal damping coefficients while C_{xy} and C_{yx} are the bearing cross coupling damping coefficients.

The state of motion of the dynamical system under consideration is completely defined by the eight state variables x_1, y_1, x_2, y_2, x, y, θ, and ϕ. However, it is seen from geometry of the system in Fig. 4 that

$$\begin{aligned} x_1 &= x-\frac{l}{2}\theta, \\ x_2 &= x+\frac{l}{2}\theta, \\ y_1 &= y-\frac{l}{2}\phi, \\ y_2 &= y+\frac{l}{2}\phi. \end{aligned} \tag{8}$$

Therefore, the previous relations in Eq. (8) reduce the state variables necessary to define the system to the four state variables (or generalized coordinates), x, y, θ and ϕ. The energy functions V and D can then be rewritten in terms of the four generalized coordinates of the system as

$$\begin{aligned} V &= \frac{1}{2}\left\{\left[K_{x_1x_1}\left(x-\frac{l}{2}\theta\right)^2+K_{x_1y_1}\left(x-\frac{l}{2}\theta\right)\left(y-\frac{l}{2}\phi\right)+\right.\right. \\ &\quad \left.\left. K_{y_1x_1}\left(y-\frac{l}{2}\phi\right)\left(x-\frac{l}{2}\theta\right)+K_{y_1y_1}\left(y-\frac{l}{2}\phi\right)^2\right]+\right. \end{aligned}$$

$$\left[K_{x_2x_2}\left(x+\frac{l}{2}\theta\right)^2+K_{x_2y_2}\left(x+\frac{l}{2}\theta\right)\left(y+\frac{l}{2}\phi\right)+ K_{y_2x_2}\left(y+\frac{l}{2}\phi\right)\left(x+\frac{l}{2}\theta\right)+K_{y_2y_2}\left(y+\frac{l}{2}\phi\right)^2\right]\Bigg\} \tag{9}$$

and

$$\begin{aligned} D \;=\; & \frac{1}{2}\Bigg\{\left[C_{x_1x_1}\left(\dot{x}-\frac{l}{2}\dot{\theta}\right)^2+C_{x_1y_1}\left(\dot{x}-\frac{l}{2}\dot{\theta}\right)\left(\dot{y}-\frac{l}{2}\dot{\phi}\right)+ C_{y_1x_1}\left(\dot{y}-\frac{l}{2}\dot{\phi}\right)\left(\dot{x}-\frac{l}{2}\dot{\theta}\right)+C_{y_1y_1}\left(\dot{y}-\frac{l}{2}\dot{\phi}\right)^2\right]+ \\ & \left[C_{x_2x_2}\left(\dot{x}+\frac{l}{2}\dot{\theta}\right)^2+C_{x_2y_2}\left(\dot{x}+\frac{l}{2}\dot{\theta}\right)\left(\dot{y}+\frac{l}{2}\dot{\phi}\right)+ C_{y_2x_2}\left(\dot{y}+\frac{l}{2}\dot{\phi}\right)\left(\dot{x}+\frac{l}{2}\dot{\theta}\right)+C_{y_2y_2}\left(\dot{y}+\frac{l}{2}\dot{\phi}\right)^2\right]\Bigg\} \end{aligned} \tag{10}$$

3. System equations of motion

Lagrange's equations:

$$\frac{d}{dt}\left(\frac{\partial T}{\partial \dot{q}_i}\right)-\frac{\partial T}{\partial q_i}+\frac{\partial V}{\partial q_i}=Q_i\,,\quad i=1,2,\ldots,n\,, \tag{11}$$

in which $Q_i=-\frac{\partial D}{\partial q_i}$ are used to derive the following set of 4 coupled, nonlinear, second order differential equations of motion of the investigated system:

$$\begin{aligned} & \Big\{M(\ddot{x}+y\theta\ddot{\phi})\Big\}+\Big\{-M\left[x(\Omega^2+\dot{\theta}^2+2\Omega\dot{\phi}\theta-2\Omega\dot{\theta}\phi)+y(\Omega\dot{\theta}\theta+\Omega\dot{\phi}\phi)\right]\Big\}+ \\ & \qquad\qquad \Big\{-2M\dot{y}(\Omega+\dot{\phi}\theta)\Big\}+ \\ & \frac{1}{2}\Bigg\{\left[2K_{x_1x_1}\left(x-\frac{l}{2}\theta\right)+K_{x_1y_1}\left(y-\frac{l}{2}\phi\right)+K_{y_1x_1}\left(y-\frac{l}{2}\phi\right)\right]+ \\ & \qquad \left[2K_{x_2x_2}\left(x+\frac{l}{2}\theta\right)+K_{x_2y_2}\left(y+\frac{l}{2}\phi\right)+K_{y_2x_2}\left(y+\frac{l}{2}\phi\right)\right]\Bigg\}+ \\ & \frac{1}{2}\Bigg\{\left[2C_{x_1x_1}\left(\dot{x}-\frac{l}{2}\dot{\theta}\right)+C_{x_1y_1}\left(\dot{y}-\frac{l}{2}\dot{\phi}\right)+C_{y_1x_1}\left(\dot{y}-\frac{l}{2}\dot{\phi}\right)\right]+ \\ & \qquad \left[2C_{x_2x_2}\left(\dot{x}+\frac{l}{2}\dot{\theta}\right)+C_{x_2y_2}\left(\dot{y}+\frac{l}{2}\dot{\phi}\right)+C_{y_2x_2}\left(\dot{y}+\frac{l}{2}\dot{\phi}\right)\right]\Bigg\} \;=\; 0\,, \end{aligned} \tag{12}$$

$$\begin{aligned} & \Big\{M(\ddot{y}+x\theta\ddot{\phi})\Big\}+\Big\{-M\left[y(\Omega^2+\dot{\phi}^2)+x(\Omega\theta\dot{\theta}+\Omega\phi\dot{\phi}-2\dot{\theta}\dot{\phi})\right]\Big\}+ \\ & \qquad\qquad \Big\{2M\dot{x}(\Omega+\dot{\phi}\theta)\Big\}+ \\ & \frac{1}{2}\Bigg\{\left[2K_{y_1y_1}\left(y-\frac{l}{2}\phi\right)+K_{x_1y_1}\left(x-\frac{l}{2}\theta\right)+K_{y_1x_1}\left(x-\frac{l}{2}\theta\right)\right]+ \end{aligned}$$

$$\left[2K_{y_2y_2}\left(x+\frac{l}{2}\phi\right)+K_{x_2y_2}\left(x+\frac{l}{2}\theta\right)+K_{y_2x_2}\left(x+\frac{l}{2}\theta\right)\right]\Big\}+ \tag{13}$$
$$\frac{1}{2}\left\{\left[2C_{y_1y_1}\left(\dot{y}-\frac{l}{2}\dot{\phi}\right)+C_{x_1y_1}\left(\dot{x}-\frac{l}{2}\dot{\theta}\right)+C_{y_1x_1}\left(\dot{x}-\frac{l}{2}\dot{\theta}\right)\right]+\right.$$
$$\left.\left[2C_{y_2y_2}\left(\dot{y}+\frac{l}{2}\dot{\phi}\right)+C_{x_2y_2}\left(\dot{x}+\frac{l}{2}\dot{\theta}\right)+C_{y_2x_2}\left(\dot{x}+\frac{l}{2}\dot{\theta}\right)\right]\right\} = 0\,,$$

$$\left\{M(x^2\ddot{\theta}-xy\ddot{\phi})+J_d\ddot{\theta}\right\}-\left\{J_p\Omega\dot{\phi}+2Mx^2\Omega\dot{\phi}\right\}+$$
$$\left\{M\left[x(\Omega\dot{y}\theta-2\Omega\dot{x}\phi+2\dot{\theta}\dot{x}-2\dot{\phi}\dot{y})+y\Omega\dot{x}\theta\right]\right\}+$$
$$\frac{1}{2}\left\{\left[-K_{x_1x_1}\left(x-\frac{l}{2}\theta\right)l-K_{x_1y_1}\left(y-\frac{l}{2}\phi\right)\frac{l}{2}-K_{y_1x_1}\left(y-\frac{l}{2}\phi\right)\frac{l}{2}\right]+\right.$$
$$\left.\left[K_{x_2x_2}\left(x+\frac{l}{2}\theta\right)l+K_{x_2y_2}\left(y+\frac{l}{2}\phi\right)\frac{l}{2}+K_{y_2x_2}\left(y+\frac{l}{2}\phi\right)\frac{l}{2}\right]\right\}+ \tag{14}$$
$$\frac{1}{2}\left\{\left[-C_{x_1x_1}\left(\dot{x}-\frac{l}{2}\dot{\theta}\right)l-C_{x_1y_1}\left(\dot{y}-\frac{l}{2}\dot{\phi}\right)\frac{l}{2}-C_{y_1x_1}\left(\dot{y}-\frac{l}{2}\dot{\phi}\right)\frac{l}{2}\right]+\right.$$
$$\left.\left[C_{x_2x_2}\left(\dot{x}+\frac{l}{2}\dot{\theta}\right)l+C_{x_2y_2}\left(\dot{y}+\frac{l}{2}\dot{\phi}\right)\frac{l}{2}+C_{y_2x_2}\left(\dot{y}+\frac{l}{2}\dot{\phi}\right)\frac{l}{2}\right]\right\} = 0\,,$$

$$\left\{M(y^2\ddot{\phi}-xy\ddot{\theta})+J_d\ddot{\phi}\right\}+\left\{J_p\Omega\dot{\phi}+2Mx^2\Omega\dot{\phi}\right\}+$$
$$\left\{M\left[y(\Omega\dot{x}\phi+2\dot{\phi}\dot{y}-2\dot{\theta}\dot{x})+x(\Omega\dot{y}\phi+2\Omega\dot{x}\theta)\right]\right\}-\{M(y\ddot{x}\theta-x\ddot{y}\theta)\}+$$
$$\frac{1}{2}\left\{\left[-K_{x_1y_1}\left(x-\frac{l}{2}\theta\right)\frac{l}{2}-K_{y_1x_1}\left(x-\frac{l}{2}\theta\right)\frac{l}{2}-K_{y_1y_1}\left(y-\frac{l}{2}\phi\right)\frac{l}{2}\right]+\right.$$
$$\left.\left[K_{x_2y_2}\left(x+\frac{l}{2}\theta\right)\frac{l}{2}+K_{y_2x_2}\left(x+\frac{l}{2}\theta\right)\frac{l}{2}+K_{y_2y_2}\left(y+\frac{l}{2}\phi\right)l\right]\right\}+ \tag{15}$$
$$\frac{1}{2}\left\{\left[-C_{x_1y_1}\left(\dot{x}-\frac{l}{2}\dot{\theta}\right)\frac{l}{2}-C_{y_1y_1}\left(\dot{y}-\frac{l}{2}\dot{\phi}\right)l-C_{y_1x_1}\left(\dot{x}-\frac{l}{2}\dot{\theta}\right)\frac{l}{2}\right]+\right.$$
$$\left.\left[C_{x_2y_2}\left(\dot{x}+\frac{l}{2}\dot{\theta}\right)\frac{l}{2}+C_{y_2x_2}\left(\dot{x}+\frac{l}{2}\dot{\theta}\right)\frac{l}{2}+C_{y_2y_2}\left(\dot{y}+\frac{l}{2}\dot{\phi}\right)l\right]\right\} = 0\,,$$

where $M = m + m^*$, $J_d = I_d + I_d^*$, and $J_p = I_p + I_p^*$.

4. Stability analysis

It is clear that derived governing equations of motion of the system: (12)–(15) are impossible to be solved analytically. However, linearizing the equations and assuming similar bearings, i.e.,

$$K_{x_1x_1} = K_{x_2x_2} = \frac{1}{2}K_{xx}\,,$$
$$K_{y_1y_1} = K_{y_2y_2} = \frac{1}{2}K_{yy}\,,$$

$$\begin{aligned} K_{x_1y_1} &= K_{y_1x_1} = \frac{1}{2}K_{xy}\,, \\ K_{x_2y_2} &= K_{y_2x_2} = \frac{1}{2}K_{yx}\,, \end{aligned} \tag{16}$$

will not only simplify the equations but also decouple them into the following two sets of equations:

$$\begin{aligned} M\ddot{x} + C_{xx}\dot{x} + \left(K_{xx} - \Omega^2 M\right) x + \left(C_{xy} - 2\Omega M\right)\dot{y} + K_{xy}y &= 0 \\ M\ddot{y} + C_{yy}\dot{y} + \left(K_{yy} - \Omega^2 M\right) y + \left(C_{yx} - 2\Omega M\right)\dot{x} + K_{yx}x &= 0 \end{aligned} \tag{17}$$

$$\begin{aligned} J_d\ddot{\theta} + l^2C_{xx}\dot{\theta} + l^2K_{xx}\theta + \left(l^2C_{xy} - \Omega J_p\right)\dot{\phi} + l^2K_{xy}\phi &= 0 \\ J_d\ddot{\phi} + l^2C_{yy}\dot{\phi} + l^2K_{yy}\phi + \left(l^2C_{yx} + \Omega J_p\right)\dot{\theta} + l^2K_{yx}\theta &= 0 \end{aligned} \tag{18}$$

It is then clear that Eqs. (17) represent the translational modes of motion (i.e. corresponding to the translational displacements x and y), whereas Eqs. (18) are the system rotational modes of motion (i.e. corresponding to the rotational displacements θ and ϕ).

The assumption of a complementary solution to equations (17) and (18) of the form $x = X\mathrm{e}^{\lambda t}$, $y = Y\mathrm{e}^{\lambda t}$, $\theta = \Theta\mathrm{e}^{\lambda t}$ and $\phi = \Phi\mathrm{e}^{\lambda t}$ leads to the following equations

$$\begin{aligned} \left(M\lambda^2 + C_{xx}\lambda + K_{xx} - \Omega^2 M\right) X + \left(C_{xy}\lambda - 2\Omega M\lambda + K_{xy}\right) Y &= 0 \\ \left(M\lambda^2 + C_{yy}\lambda + K_{yy} - \Omega^2 M\right) Y + \left(C_{yx}\lambda + 2\Omega M\lambda + K_{yx}\right) X &= 0\,, \end{aligned} \tag{19}$$

$$\begin{aligned} \left(J_d\lambda^2 + l^2C_{xx}\lambda + l^2K_{xx}\right)\Theta + \left(l^2C_{xy}\lambda - \Omega J_p\lambda + l^2K_{xy}\right)\Phi &= 0 \\ \left(J_d\lambda^2 + l^2C_{yy}\lambda + l^2K_{yy}\right)\Phi + \left(l^2C_{yx}\lambda + \Omega J_p\lambda + l^2K_{yx}\right)\Theta &= 0\,, \end{aligned} \tag{20}$$

The system of equations (19) and (20) can be put on the matrix form

$$[A]\{X_i\} = 0\,, \tag{21}$$

where $[A]$ is the coefficient matrix and $\{X_i\} = [X, Y, \Theta, \Phi]^T$.

The characteristic equation $\det[A] = 0$ leads to the following eight's order algebraic equations

$$\begin{aligned} \big\{\left[M\lambda^2 + C_{xx}\lambda + K_{xx} - \Omega^2 M\right]\left[M\lambda^2 + C_{yy}\lambda + K_{yy} - \Omega^2 M\right] - \\ \left[C_{xy}\lambda - 2\Omega M\lambda + K_{xy}\right]\left[C_{yx}\lambda + 2\Omega M\lambda + K_{yx}\right]\big\} \\ \big\{\left[J_d\lambda^2 + l^2C_{xx}\lambda + l^2K_{xx}\right]\left[J_d\lambda^2 + l^2C_{yy}\lambda + l^2K_{yy}\right] - \\ \left[l^2C_{xy}\lambda - \Omega^2 J_p\lambda + l^2K_{xy}\right]\left[l^2C_{yx}\lambda + \Omega^2 J_p\lambda + l^2K_{yx}\right]\big\} &= 0\,. \end{aligned} \tag{22}$$

It is clear that the system characteristic equation (22) can be slitted into the following two fourth order characteristic equations:

$$\begin{aligned} \left[M\lambda^2 + C_{xx}\lambda + K_{xx} - \Omega^2 M\right]\left[M\lambda^2 + C_{yy}\lambda + K_{yy} - \Omega^2 M\right] - \\ \left[C_{xy}\lambda - 2\Omega M\lambda + K_{xy}\right]\left[C_{yx}\lambda + 2\Omega M\lambda + K_{yx}\right] &= 0\,, \\ \left[J_d\lambda^2 + l^2C_{xx}\lambda + l^2K_{xx}\right]\left[J_d\lambda^2 + l^2C_{yy}\lambda + l^2K_{yy}\right] - \\ \left[l^2C_{xy}\lambda - \Omega J_p\lambda + l^2K_{xy}\right]\left[l^2C_{yx}\lambda + \Omega J_p\lambda + l^2K_{yx}\right] &= 0\,. \end{aligned} \tag{23}$$

Thus, the first of Eqs (23) represents the characteristic equation of the translational modes of motion, or simply the translational characteristic equation, whereas the secon one represents the rotational characteristic equation.

5. Conditions of stability of system translational modes of motion

The translational characteristic equation (the first of Eq. (23)) can be put on the form

$$\sum_{i=0}^{4} A_i \lambda^{4-i} = 0\,. \tag{24}$$

The Routh-Hurwitz stability array is given by

$$\begin{vmatrix} A_1 & A_0 & 0 & 0 \\ A_3 & A_2 & A_1 & A_0 \\ 0 & A_4 & A_3 & A_2 \\ 0 & 0 & 0 & A_4 \end{vmatrix} \tag{25}$$

According to the R-H stability criterion, the necessary and sufficient conditions of asymptotic stability are that all of the determinants Δ_i must be positive definite, i.e.,

$$\begin{aligned}
\Delta_1 &= A_1 = M(C_{xx}+C_{yy}) > 0\,,\\
\Delta_2 &= A_1A_2 - A_0A_3 = M(C_{xx}+C_{yy})\left[M(K_{yy}-\Omega^2M)+M(K_{xx}-\Omega^2M)+\right.\\
&\quad C_{xx}C_{yy}-(C_{xy}-2\Omega M)(C_{yx}+2\Omega M)] - M^2\left[C_{xx}(K_{yy}-\Omega^2M)+\right.\\
&\quad \left.C_{yy}(K_{xx}-\Omega^2M)-K_{yx}(C_{xy}-2\Omega M)-K_{xy}(C_{yx}+2\Omega M)\right] > 0\,,\\
\Delta_3 &= A_3\{A_1A_2-A_0A_3\}-A_4\{A_1^2\}\\
&\quad \left[C_{xx}(K_{yy}-\Omega^2M)+C_{yy}(K_{xx}-\Omega^2M)-K_{yx}(C_{xy}-2\Omega M)-\right.\\
&\quad K_{xy}(C_{yx}-2\Omega M)]\left\{\left[M^2(C_{xx}+C_{yy})(K_{xx}+K_{yy}-2\Omega^2M)+\right.\right.\\
&\quad \left.MC_{xx}C_{yy}(C_{xx}+C_{yy})-M(C_{xy}-2\Omega M)(C_{yx}+2\Omega M)(C_{xx}+C_{yy})\right]\\
&\quad -M^2\left[C_{xx}(K_{yy}-\Omega^2M)+C_{yy}(K_{xx}-\Omega^2M)-K_{yx}(C_{xy}-2\Omega M)-\right.\\
&\quad \left.\left.K_{xy}(C_{yx}+2\Omega M)]\right\}-\right.\\
&\quad M^2(C_{xx}+C_{yy})^2\left[(K_{xx}-\Omega^2M)(K_{yy}-\Omega^2M)-K_{xy}K_{yx}\right] > 0\,,\\
\Delta_4 &= A_4\Delta_3 > 0\,,
\end{aligned}$$

which implies that $A_4 > 0$, i.e.,

$$\left(K_{xx}-\Omega^2M\right)\left(K_{yy}-\Omega^2M\right)-K_{xy}K_{yx} > 0\,. \tag{26}$$

The first condition Eq. (26) is trivial since M, C_{xx}, C_{yy} are always positive definite. However, from the rest of the conditions one can deduce the following set of nontrivial conditions of stability after being nondimensionalized:

$$\begin{aligned}
\left(\frac{\omega_{xx}^2}{\Omega^2}-1\right)\left(\frac{\omega_{yy}^2}{\Omega^2}-1\right) &> \frac{\omega_{xy}^2\omega_{yx}^2}{\Omega^4}\\
\alpha_{xx}\left(\frac{\omega_{yy}^2}{\Omega^2}-1\right)+\alpha_{yy}\left(\frac{\omega_{xx}^2}{\Omega^2}-1\right) &> \frac{\omega_{xy}^2}{\Omega^2}(\alpha_{yx}+1)+\frac{\omega_{yx}^2}{\Omega^2}(\alpha_{xy}-1)\\
\left(\frac{\omega_{xx}^2}{\Omega^2}-1\right)+\left(\frac{\omega_{yy}^2}{\Omega^2}-1\right) &> 4\left[(\alpha_{xy}-1)(\alpha_{yx}+1)-\alpha_{xx}\alpha_{yy}\right]
\end{aligned} \tag{27}$$

where $\omega_{rs}^2 = \frac{K_{rs}}{M}$ and $\alpha_{rs} = \frac{C_{rs}}{2\Omega M}$ in which r and s stand for x or y.

6. Effect of various end support parameters on system stability regions

Based on conditions (27), the system stability boundaries are presented graphically in terms of the various system nondimensionalized parameters as shown in Figs. 5 to 10.

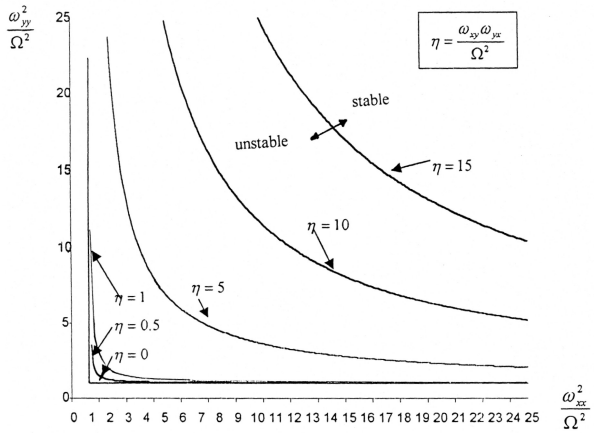

Figure 5 Effect of cross-coupling stiffness parameter η on stability regions

The first of conditions (28) is represented graphically in Fig. 5 which illustrates the system stability boundaries in terms of the dimensionless cross coupling stiffness parameter $\eta = \frac{\omega_{xy}\omega_{yx}}{\Omega^2}$. The figure clearly shows that the greater the magnitude of η, the smaller the region of stability. Thus, Fig. 5 demonstrates the significance of the bearing cross-coupling stiffness as an essential factor of system instability.

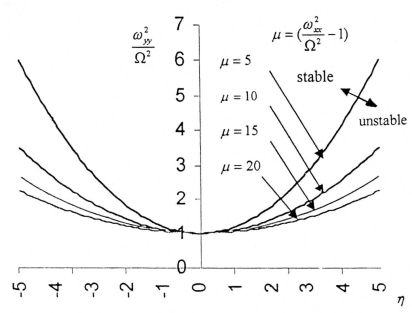

Figure 6 Effect of principal stiffness parameter μ on stability regions

Fig. 6 is drawn based on the first of conditions (28) also where the stability boundaries are drawn here in terms of the dimensionless principal stiffness parameter $\mu = \left(\frac{\omega_{xx}^2}{\Omega^2} - 1\right)$. It can be easily seen from this Figure, that the region of stability grow with the increase in value of μ. The maximum stability region is found when μ tends to infinity (i.e., case of rigid end support) where stability region tends to be the entire plan above the common tangential horizontal line $\frac{\omega_{yy}^2}{\Omega^2} = 1$. This emphasize the intuitive expectation that the increase of end supports principal enhances system stability.

To study the effect of end support damping anisotropy on system stability regions, let us consider the second of conditions (28) in case of zero cross coupling parameters. In this case it reduces to

$$\alpha_{xx}\left(\frac{\omega_{yy}^2}{\Omega^2} - 1\right) + \alpha_{yy}\left(\frac{\omega_{xx}^2}{\Omega^2} - 1\right) > 0\,. \tag{28}$$

Denoting $\nu = \frac{\alpha_{yy}}{\alpha_{xx}} = \frac{C_{yy}}{C_{xx}}$ as dimensionless anisotropic damping parameter, the second condition can be rewritten as

$$\frac{\omega_{yy}^2}{\Omega^2} + \nu\frac{\omega_{xx}^2}{\Omega^2} > 1 + \nu\,, \tag{29}$$

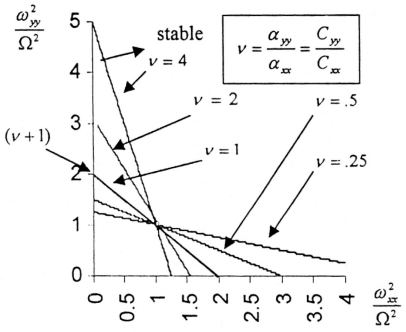

Figure 7 Effect of anisotropic damping parameter ν on stability regions

Thus, the stability boundaries, drawn in terms of ν, may be represented by either a family of straight lines (Fig. 7) whose equation given by

$$\frac{\omega_{yy}^2}{\Omega^2} + \nu\frac{\omega_{xx}^2}{\Omega^2} = 1 + \nu\,, \tag{30}$$

or a family of ellipses (Fig. 8) whose equation is given by

$$\frac{\frac{\omega_{xx}^2}{\Omega^2}}{1 + \frac{1}{\nu}} + \frac{\frac{\omega_{yy}^2}{\Omega^2}}{1 + \nu} = 1\,. \tag{31}$$

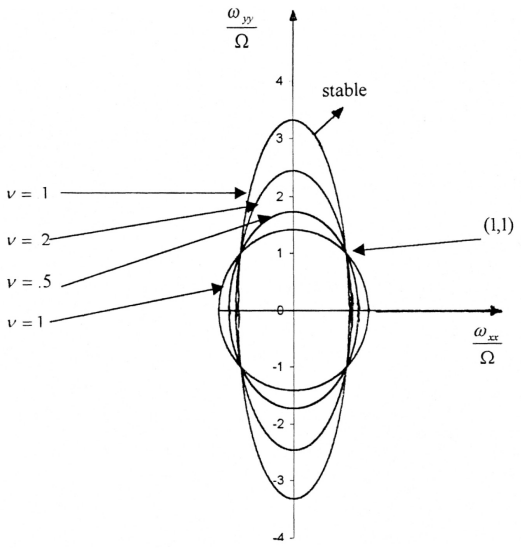

Figure 8 Effect of ν on stability regions

In Fig. 7, the region under each straight line is unstable whereas the upper portion is stable. Like wise, the area inside each ellipse in Fig. 8 represents an instability regions. Therefore, the stability boundaries presented in Fig. 7 and 8 share the common characteristic that

(a) the minimum instability region corresponds to the isotropic damping $\nu = 1$,

(b) the instability regions grow with the increase of deviation from the isotropic damping case $\nu = 1$, and,

(c) the large instability regions occur at the two extreme anisotropic damping case $\nu \to 0$ and $\nu \to \infty$.

Thus, the results extracted from Fig. 3 or 4 clearly demonstrate the role played by the anisotropy of bearing damping coefficients as one of the sources of whirling instability of rotor bearing systems.

Now, if the cross coupling parameters are taken into consideration, then the second of the conditions (28) rewritten as

$$\frac{\omega_{yy}^2}{\Omega^2} + \nu\frac{\omega_{xx}^2}{\Omega^2} > 1 + \nu + \frac{Q}{\alpha_{xx}}\,, \tag{32}$$

where

$$Q = \frac{\omega_{xy}^2}{\Omega^2}(\alpha_{yx} + 1) + \frac{\omega_{yx}^2}{\Omega^2}(\alpha_{xy} - 1)\,,$$

can be used to study the influence of Q and α_{xx} s on the stability boundaries shown before in Fig. 7 or 8. According to the second of conditions (28), the instability

regions shown before in Fig. 3 are going to grow, where the points of intersection of each stability curve with the horizontal and vertical axes should extend to the points $\left(1+\frac{1}{\nu}+\frac{Q}{\nu\alpha_{xx}},0\right)$ and $\left(0,1+\nu+\frac{Q}{\alpha_{xx}}\right)$ respectively as illustrated in Fig. 9. Like wise, the instability regions in Fig. 8 should be enlarged, where the length of the horizontal and vertical axis of each ellipse is going to increase to

$$2\sqrt{1+\frac{1}{\nu}+\frac{Q}{\nu\alpha_{xx}}}$$

and

$$2\sqrt{1+\nu+\frac{Q}{\alpha_{xx}}}\,,$$

respectively. This indicates that when the bearing cross coupling a stiffness and damping parameters contained in Q are taken into consideration, the instability region grow. Thus, it has been shown that the bearing cross coupling stiffness and damping parameters are sources of whirling instability, while the principal damping parameters enhance system whirling stability.

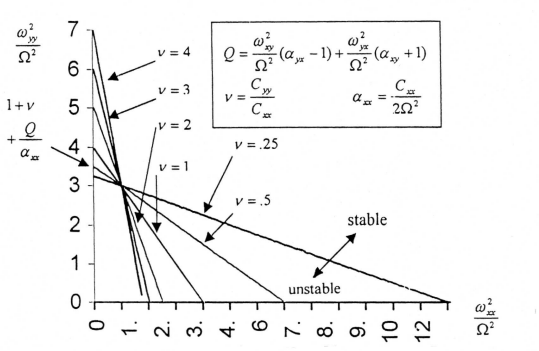

Figure 9 Effect of Q and α_{xx} on stability regions

Lastly, the third of conditions (28) is used to investigate the effect of each of the principal and the cross coupling damping parameter of the bearings (or the two end supports in general) on the system whirling stability. In case of no cross coupling, the condition reduces to

$$\left(\frac{\omega_{xx}^2}{\Omega^2}-1\right)+\left(\frac{\omega_{yy}^2}{\Omega^2}-1\right)+4\beta>0\,, \tag{33}$$

where β is a non dimensional principal damping parameter defined by $\beta=\alpha_{xx}\alpha_{yy}$. Stability boundaries drawn in terms of β in Fig. 10 represent a family of coaxial circles.

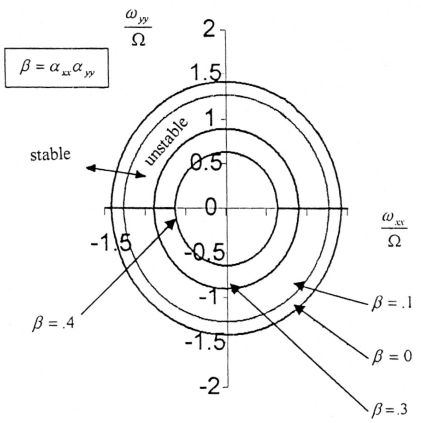

Figure 10 Effect of principal damping parameter β on stability regions

In Fig. 10, it is easy to observe that the circles with higher value of β lead to smaller instability regions. However, if the cross coupling damping is considered, then the family of stability boundaries in Fig. 10 is going to grow since its equation becomes

$$\left(\frac{\omega_{xx}}{\Omega}\right)^2 + \left(\frac{\omega_{yy}}{\Omega}\right)^2 + 4\beta = 2 + 4\gamma\,, \tag{34}$$

where γ is the dimensionless cross coupling parameter $(\alpha_{xy}-1)(\alpha_{yx}+1)$. It is then evident that the larger the values of γ, the larger the regions of instability. Thus, based on the third of conditions (28), it has been shown that the stability regions grow with increasing β and decreasing γ. This emphasizes the results reached before in this investigation that the two end support cross coupling parameters can be significant sources of instability, whereas the principal parameters are sources of enhancing stability.

7. Conditions of stability of system rotational modes of motion

It is clear that the rotational characteristic equation (the second of Eqs (23)) is analogous to the previously studied translational characteristic – the first of Eqs (23). Therefore, following the same previously mentioned steps, one can reach to the following nontrivial conditions for stability of system rotational modes of motion.

$$\begin{aligned}
\omega_{xx}^2\omega_{yy}^2 &> \omega_{xy}^2\omega_{yx}^2 \\
\alpha'_{xx}\frac{\omega'^2_{yy}}{\Omega^2} + \alpha'_{yy}\frac{\omega'^2_{xx}}{\Omega^2} &> \frac{\omega'^2_{xy}}{\Omega^2}(\alpha'_{yx}-1) + \frac{\omega'^2_{yx}}{\Omega^2}(\alpha'_{xy}+1) \\
\alpha_{xx}\alpha_{yy} + \frac{\omega_{xx}^2}{\Omega^2} + \frac{\omega_{yy}^2}{\Omega^2} &> \alpha_{xy}\alpha_{yx} + \frac{J_p}{J_d}(\alpha_{xy}-\alpha_{yx}) - \left(\frac{J_p}{J_d}\right)^2\,,
\end{aligned} \tag{35}$$

in which the following nondimensional quantities are defined:

$$\begin{aligned}
\frac{\omega_{ij}^2}{\Omega^2} &= \frac{l^2K_{ij}}{\Omega^2 J_d} \quad \alpha_{ij} = \frac{l^2C_{ij}}{\Omega J_d} \\
\frac{\omega'^2_{ij}}{\Omega^2} &= \frac{l^2K_{ij}}{\Omega^2 J_p} \quad \alpha'_{ij} = \frac{l^2C_{ij}}{\Omega J_p}
\end{aligned}$$

where i and j stand for x or y.

8. Effect of various end support parameters on system stability regions

Based on conditions (35), the system stability boundaries are presented graphically in terms of the various system nondimensionalized parameters as shown in Fig. 11 through 14.

The first of conditions (35) is represented graphically in Fig. 11, where the stability boundaries are drawn in terms of the nondimensionatized cross coupling stiffness parameter $\eta = \frac{\omega_{xy}\omega_{yx}}{\Omega^2}$. The stability curves represent a family of rectangular hyperbolas given by the equation

$$\frac{\omega_{xx}^2}{\Omega^2}\frac{\omega_{yy}^2}{\Omega^2} = \eta^2\,, \tag{36}$$

with $\frac{\omega_{xx}^2}{\Omega^2} = 0$ and $\frac{\omega_{yy}^2}{\Omega^2} = 0$ as asymptotic lines. The area under each curve (the lower region) is unstable, white the inside portion (the upper region) is stable. The figure clearly shows that the greater the magnitude of η, the smaller the region of stability. The maximum stability region is obtained when η is zero where the stability region is the entire area bounded by the two asymptotes. Therefore, Fig. 11 demonstrates clearly the significance of the bearing cross coupling stiffness parameter η at an essential factor of system instability.

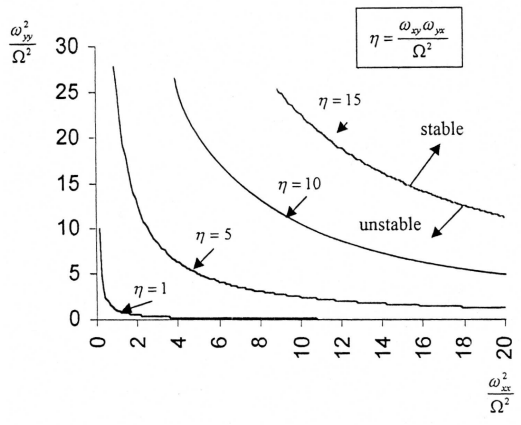

Figure 11 Effect of cross-coupling stiffness parameter η on stability regions

From the first of conditions (36), one can also show the influence of principal (direct) stiffness coefficient on the stability regions if $\frac{\omega_{xx}^2}{\Omega^2}$ or $\frac{\omega_{yy}^2}{\Omega^2}$ is taken as a parameter. Let us take $\frac{\omega_{xx}^2}{\Omega^2}$ as a parameter denoted by μ. The stability boundaries,

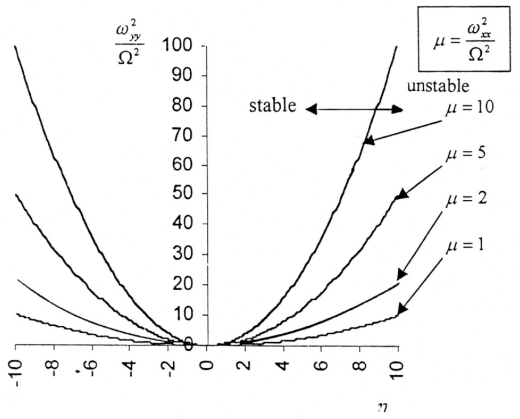

Figure 12 Effect of principal stiffness parameter μ on stability regions

drawn in terms of μ, are then represented by the family of parabolas

$$\eta^2 = \nu \frac{\omega_{yy}^2}{\Omega^2} \tag{37}$$

which is shown in Fig. 12. It can be easily seen from Fig. 12 that the region of stability grow with the increase in variable μ. The maximum stability region is found when μ tends to infinity (rigid end support), where the stability region tends to be the entire plan above the common tangential horizontal line $\frac{\omega_{yy}^2}{\Omega^2} = 0$. This emphasize the intuitive expectation that the increase of end supports principal stiffness enhance the system stability.

To study the effect of end support damping anisotropy on the system stability regions, let us consider the second of conditions (36) in the form

$$\frac{\omega'^2_{yy}}{\Omega^2} + \nu \frac{\omega'^2_{xx}}{\Omega^2} > \frac{Q'^2}{\alpha'^2_{xx}} \tag{38}$$

where

$$Q' = \frac{\omega'^2_{xy}}{\Omega^2}(\alpha'_{yx} - 1) + \frac{\omega'^2_{yx}}{\Omega^2}(\alpha'_{xy} + 1)\,,$$

and

$$\nu = \frac{\alpha'_{yy}}{\alpha'_{xx}} = \frac{C_{yy}}{C_{xx}}\,.$$

This condition is represented graphically in Fig. 13. The results presented in Fig. 13 show the influence of Q' and α'_{xx} on the stability boundaries.

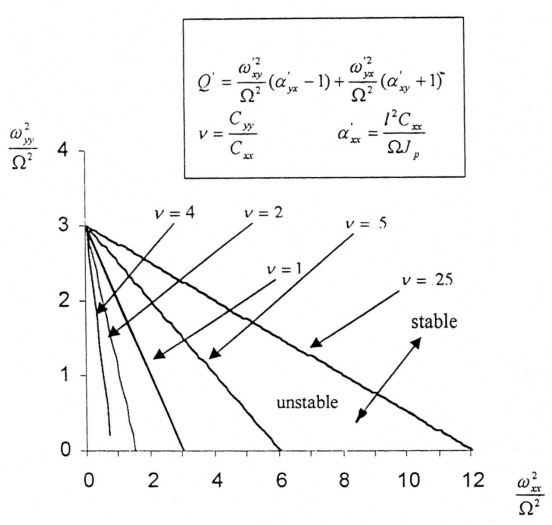

Figure 13 Effect of Q', α'_{xx} and anisotropic parameter ν on stability regions

Lastly, the third of conditions (36) is used to investigate the effect of each of the principal and the cross-coupling damping parameters of the bearings on the system whirling stability. Let us put it in the form:

$$\beta + \frac{\omega_{xx}^2}{\Omega^2} + \frac{\omega_{yy}^2}{\Omega^2} > \gamma \tag{39}$$

where

$$\gamma = \alpha_{xy}\alpha_{yx} + \frac{J_p}{J_d}(\alpha_{xy} - \alpha_{yx}) - \left(\frac{J_p}{J_d}\right)^2 ,$$

and

$$\beta = \alpha_{xx}\alpha_{yy} .$$

Thus, the stability boundaries are drawn in terms of β in Fig. 14, it represents a family of coaxial circles whose equations are

$$\frac{\omega_{xx}^2}{\Omega^2} + \frac{\omega_{yy}^2}{\Omega^2} + \beta = \gamma , \tag{40}$$

Fig. 14 shows that the stability regions grow with increasing β and decreasing γ.

9. Summary and Conclusions

The differential equations governing the motion of a rotor-bearing system modeled as an axially symmetric appendage at the mid span of a rotating rigid shaft mounted on two dissimilar 8-coefficient bearings is derived using Lagrange's equations. Linearization of the governing equations of motion of the system in case of similar bearings decouples the equation of motion of the system to two distinct sets of equations corresponding to the translational and rotational modes of motion. The well known method of R-H stability criterion was applied on both the

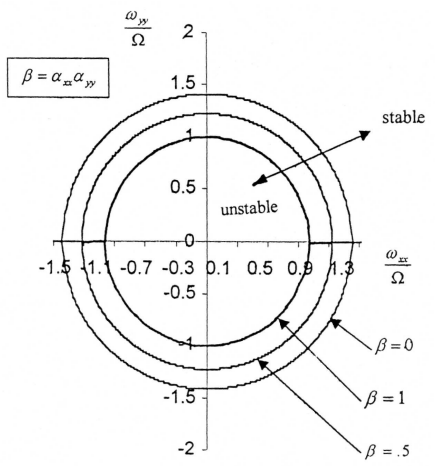

Figure 14 Effect of principal damping parameter β on stability regions

characteristic equations of the translational and rotational modes of motion and sufficient conditions of asymptotic stability in terms of the system nondimensionalized parameters have been obtained in each mode. The stability regions were then represented graphically as functions of the system nondimensionalized parameters and thorough analysis of the role played by each parameter in affecting the stability of whirling motion of the system is presented.

Among the results reached in this study, the following concluding remarks can be stated:

1. The graphs of the stability boundaries in terms of the nondimensionalized system parameters presented in this study are typical examples of the types of primitive design information available to engineers through the equations provided in this investigation.

2. The anisotropy of bearing damping coefficients is a source of whirl instability of rotor-bearing systems where the maximum stability regions occur in the isotropic damping case ($C_{xx} = C_{yy}$), whereas the instability regions grow with the increase of deviation from the isotropic damping case.

3. The bearing cross coupling stiffness and damping coefficients are serious sources of instability of the whirl motion of rotor-bearing systems.

4. The bearing principal stiffness and damping coefficients enhance the whirl stability of rotor-bearing systems.

References

[1] **Abdel-Sattar, N**: *Linear and Nonlinear Stability Analysis of Rotating Dynamical Systems with Elastic and Damped Supports*, (2002), M. Sc. Thesis, Dept. of Eng. Math. & Phys., Fac. Of Eng., Ain Shams Univ., Cairo, Egypt.

[2] **El-Marhomy, A**: On the translational whirling motion of rotor-bearing systems, *J. Int. Math & Comp. Sci. (Math. Ser.)*, (1994), **7**, 1, 73-84.

[3] **El-Marhomy, A**: On dynamic response of disk-shaft-bearing systems, *ASME. J. Modelling, Measurement & Control*, (1998), **66**, 2, 7-18.

[4] **Chivens, DR**: *The natural frequencies and critical speeds of a rotating ftexible shaft-disk system*, (1973), Ph.D. Thesis, Arizona State Univ.: Tempe, Arizona.

[5] **Kisk, RG** and **Gunter, EJ**: Transient response of rotor-bearing systems, *ASME J. Eng. for Industry*, (1964), 682-693.

[6] **Chang, CO** and **Cheng, JW**: Nonlinear Dynamics and Stability of a Rotating Shaft-Disk System, *J. Sound and Vibrations*, (1993), **160**, 3, 433-454.

[7] **Pedersen, PT**: On self excited whirl of rotors, *Ingenieur-Archiv*, (1973), **42**, 267-286.

[8] **El-Marhomy, A**: Dynamic stability of elastic rotor-bearing systems via Lyapunov's direct method, *J. Applied Mechanics*, (1991), **58**, 1056-1065.